Inorg. Chem. **2006**, *45*, 7828–7834

Iron Complexes of N-Confused Pyriporphyrin: NMR Studies

Radomir Myśliborski, Krystyna Rachlewicz, and Lechosław Latos-Grażyński*

Department of Chemistry, University of Wrocław, 14 F. Joliot-Curie Street, Wrocław 50 383, Poland

Received May 24, 2006

Insertion of iron(II) into 6,11,16,21-tetraaryl-3-aza-*m*-benziporphyrin (N-confused pyriporphyrin, (PyP*H*)H) yielded the high-spin iron(II) complex, (PyP*H*)Fe^{II}Br. The coordination of iron(II) to the perimeter nitrogen atom of (PyP*H*)-Fe^{II}Br resulted in the formation of the diiron species. Oxidation and oxygenation of (PyP*H*)Fe^{II}Br were followed by ^{1}H NMR spectroscopy. The addition of Br_2 to the solution of (PyP*H*)Fe^{II}Br in the absence of dioxygen results in a one-electron oxidation yielding the high-spin iron(III) N-confused pyriporphyrin [(PyP*H*)Fe^{III}Br]$^+$ which preserves the side-on interaction between the inverted pyridine ring and metal ion. The reaction of (PyP*H*)Fe^{II}Br with dioxygen ends up with the formation of a five-coordinate species (PyPO)Fe^{III}Br] ((PyPOH)H = 3-aza-22-hydroxy-*m*-benziporphyrin, PyPO = the corresponding dianion) which is formed by oxygenation at the C(22) position. Coordination of a metal ion by 3-aza-22-hydroxy-benziporphyrin imposes a steric constraint on the geometry of the ligand. The halide ligand of (PyPO)Fe^{III}Br coordinates on one of the two inequivalent faces of the macrocycle, leading to two distinct species: syn and anti. The ^{1}H NMR spectra of paramagnetic iron(II) and iron(III) N-confused pyriporphyrin complexes have been examined. The characteristic patterns of pyrrole and pyridine resonances have been found to be diagnostic of the ground electronic state of iron and the donor nature of the C(22)H and N(3) centers. The enormous downfield H(22) paramagnetic shift, determined for the iron(II) N-confused pyriporphyrin, provides a distinct resonance in a peculiar spectroscopic window (350–800 ppm) for a series of axial ligands which can be considered as a diagnostic sign of an agostic Fe^{II}···{C(22)–H} interaction. Coordination of the pyridine moiety via the perimeter N(3) atom is reflected unambiguously by the H(2/4) resonance at 201 ppm.

Introduction

N-confused pyriporphyrin (6,11,16,21-tetraaryl-3-aza-*m*-benziporphyrin) (PyP*H*)H **1** is the simplest homologue of N-confused 5,10,15,20-tetraarylporphyrin **3** with the supplementary carbon inserted into a pyrrolic C_α−N bond.[1] Because it is readily seen, by analogy to the porphyrin−N-confused porphyrin couple, the 3-aza-*m*-benziporphyrin **1** can be related to the regular pyriporphyrin (22-aza-*m*-benziporphyrin) **2** by application of the N-confusion concept.[2] Formally, **1** can be also constructed by replacement of one of the pyrrole rings of 5,10,15,20-tetraarylporphyrin with a pyridine moiety, linked to the macrocycle at the 3,5-position. Alternatively, the molecule can be treated as a derivative of 6,11,16,21-tetraaryl-*m*-benziporphyrin **4**,[3] where the 3-CH fragment has been replaced with a nitrogen atom (Chart 1). N-confused pyriporphyrin **1** contains the (*C*NNN) coordination core of the carbaporphyrinoids.[4−12]

In general, carbaporphyrinoids are versatile ligands, which offer a means to study metal−carbon bonding in a macrocyclic environment.[3,12−17] The coordination brings the metal

* To whom correspondence should be addressed. E-mail: LLG@wchuwr.chem.uni.wroc.pl.

(1) Myśliborski, R.; Latos-Grażyński, L. *Eur. J. Org. Chem.* **2005**, 5039.
(2) Myśliborski, R.; Latos-Grażyński, L.; Szterenberg, L. *Eur. J. Org. Chem.* **2006**, 3064.
(3) Stępień, M.; Latos-Grażyński, L. *Chem.—Eur. J.* **2001**, *7*, 5113.
(4) Lash, T. D. *Synlett* **1999**, 279.
(5) Latos-Grażyński, L. Core Modified Heteroanalogues of Porphyrins and Metalloporphyrins. In *The Porphyrin Handbook*; Kadish, K. M., Smith, K. M., Guilard, R., Eds.; Academic Press: New York, 2000; pp 361−416.
(6) Pawlicki, M.; Latos-Grażyński, L. *Chem. Rec.* **2006**, *6*, 64.
(7) Furuta, H.; Maeda, H.; Osuka, A. *Chem. Commun.* **2002**, 1795.
(8) Harvey, J. D.; Ziegler, C. J. *Coord. Chem. Rev.* **2003**, *247*, 1.
(9) Ghosh, A. *Angew. Chem., Int. Ed. Engl.* **2004**, *43*, 1918.
(10) Srinivasan, A.; Furuta, H. *Acc. Chem. Res.* **2005**, *38*, 10.
(11) Chmielewski, P. J.; Latos-Grażyński, L. *Coord. Chem. Rev.* **2005**, *249*, 2510.
(12) Stępień, M.; Latos-Grażyński, L. *Acc. Chem. Res.* **2005**, *38*, 88.
(13) Stępień, M.; Latos-Grażyński, L.; Lash, T. D.; Szterenberg, L. *Inorg. Chem.* **2001**, *40*, 6892.
(14) Stępień, M.; Latos-Grażyński, L. *J. Am. Chem. Soc.* **2002**, *124*, 3838.
(15) Stępień, M.; Latos-Grażyński, L.; Szterenberg, L.; Panek, J.; Latajka, Z. *J. Am. Chem. Soc.* **2004**, *126*, 4566.
(16) Stępień, M.; Latos-Grażyński, L.; Szterenberg, L. *Inorg. Chem.* **2004**, *43*, 6654.

10.1021/ic060906r CCC: $33.50
Published on Web 08/18/2006

Chart 1. Selected Carbaporphyrinoids and Pyriporphyrin

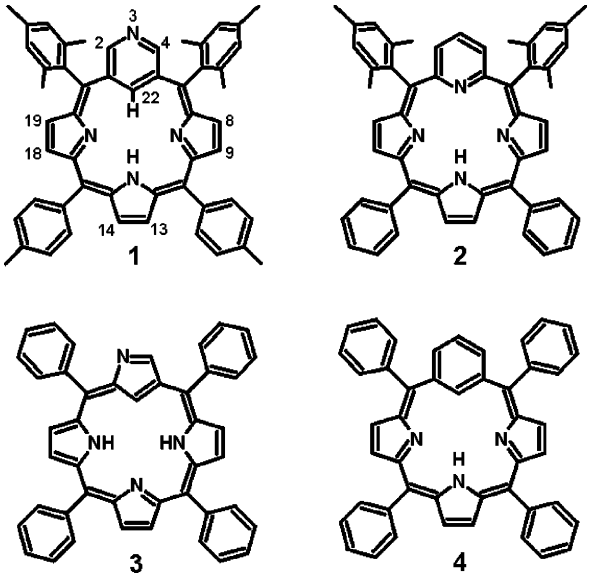

ion into the vicinity of chosen carbocycles or heterocycles, leading to activation of C−H bonds, followed by metal coordination or resulting in weak interactions, which can be spectroscopically observed.[15] A special role in this line of investigations has been played by the first discovered carbaporphyrinoid−inverted (N-confused) porphyrin.[18,19] The inverted porphyrin and its derivatives revealed a remarkable tendency to stabilize peculiar organometallic compounds.[5,7,8,10,11] Complex dimeric or oligomeric structures, involving N-confused porphyrins, linked by external coordination using the N(2) donor are of particular interest.[10,20−26] An iron(III)−N-confused porphyrin complex assembled using axially coordinated phenol and the perimeter nitrogen of the macrocycle has been recently reported.[27]

The ability of carbaporphyrinoids to coordinate metal ions and to form metal−carbon bonds extends beyond the family of N-confused porphyrins.[3,5,7,13,14,28] For this paper, the coordination properties of *m*-benziporphyrin and closely related molecules are of particular interest. To date, *m*-benziporphyrin has revealed two coordination modes. In the first one, a metal ion is bound in the macrocyclic cavity by three pyrrolic nitrogens and a trigonal carbon of the benzene ring.[13,28] The macrocyclic effect is not always sufficient to enforce the metalation of benzene. In such a case, the *m*-phenylene ring is held proximate to the metal ion without actually forming a covalent bond.[3,12,15−17]

Because the present studies are focused on the iron complexes of N-confused porphyrin, the relevant studies concerning iron carbaporphyrinoid chemistry have been briefly overviewed. Iron(II) inverted porphyrin complexes **3**-FeBr and **3**-Fe(SC_7H_7) present the conformation with the iron in a side-on position with respect to the inverted pyrrole plane.[29] The agostic iron(II)−inverted pyrrole ring interaction ($Fe^{II}\cdots C(21)-H$) is reflected in the ^{1}H NMR studies by an unprecedented isotropic shift of the engaged H(21).[30] A similar coordination mode has been determined for iron(II) *m*-benziporphyrin where the $Fe^{II}\cdots C(22)-H$ interaction was also reflected by a considerable paramagnetic shift of H(22).[17] A dimeric iron(II) N-confused porphyrin, [**3**-Fe]$_2$, was obtained from the anaerobic reaction of **3**-FeBr with NaSePh. Under aerobic conditions, a μ-hydroxo-bridged iron(III) dimer was obtained with a sodium ion bridging the outer-N atoms. Oxygenation occurred at the inner-core pyrrolic carbon to form a novel porphyrinic ring.[21] Oxidation and oxygenation of **3**-FeBr was also investigated using ^{1}H and ^{2}H NMR spectroscopy.[31] Two modes of coordination of iron(III) to the N-confused pyrrole ring (side-on and via the trigonally hybridized carbon atom) were determined. In the presence of oxygen, the formation of the C(22)O carbonyl group was established; it was involved in a direct interaction between the iron center and the π-electron density on the carbonyl group in an η^2 mode.

^{1}H NMR spectroscopy provides a uniquely useful probe for studying the structure of iron porphyrin complexes in solution.[32] The hyperfine shift patterns are particularly sensitive to the ligation, oxidation, and spin state of the metal ion. For instance, the iron(III) 2-hydroxy-5,10,15,20-tetraphenylporphyrin oligomerization yielded a ^{1}H NMR spectroscopic pattern that is unequivocally explainable in terms of a cyclic trimeric structure.[33,34] In this contribution, our investigations have been focused on iron complexes of N-confused pyriporphyrin. Three inequivalent pyrrole and two pyridyl resonances of iron complexes provided a direct probe of the spin density around the porphyrin macrocycle and allowed the detection of a diiron(II) structure. The perimeter coordination can be examined by monitoring some reactions directly by ^{1}H NMR spectroscopy without the problems inherent in separation and isolation of products.

Results and Discussion

Formation and Characterization of Iron(II) Complexes. Insertion of iron(II) into 6,11,16,21-tetraaryl-3-aza-*m*-ben-

(17) Hung, C.-H.; Chang, F.-C.; Lin, C.-Y.; Rachlewicz, K.; Stępień, M.; Latos-Grażyński, L.; Lee, G.-H.; Peng, S.-M. *Inorg. Chem.* **2004**, *43*, 4118.
(18) Chmielewski, P. J.; Latos-Grażyński, L.; Rachlewicz, K.; Głowiak, T. *Angew. Chem., Int. Ed. Engl.* **1994**, *33*, 779.
(19) Furuta, H.; Asano, T.; Ogawa, T. *J. Am. Chem. Soc.* **1994**, *116*, 767.
(20) Furuta, H.; Youfu, K.; Maeda, H.; Osuka, A. *Angew. Chem., Int. Ed.* **2003**, *42*, 2186.
(21) Hung, C.-H.; Chen, W.-C.; Lee, G.-H.; Peng, S.-M. *Chem. Commun.* **2002**, 1516.
(22) Furuta, H.; Ishizuka, T.; Osuka, A. *J. Am. Chem. Soc.* **2002**, *124*, 5622.
(23) Chmielewski, P. J.; Schmidt, I. *Inorg. Chem.* **2004**, *43*, 1885.
(24) Chmielewski, P. J. *Angew. Chem., Int. Ed.* **2005**, *44*, 6417.
(25) Maeda, H.; Furuta, H. *J. Porphyrins Phthalocyanines* **2004**, *8*, 67.
(26) Furuta, H.; Morimoto, T.; Osuka, A. *Inorg. Chem.* **2004**, *43*, 1618.
(27) Hung, C.-H.; Chang, C.-H.; Ching, W.-M.; Chuanga, C.-H. *Chem. Commun.* **2006**, 1866.
(28) Venkatraman, S.; Anand, V. G.; Pushpan, S. K.; Sankar, J.; Chandrashekar, T. K. *Chem. Commun.* **2002**, 462.
(29) Chen, W.-C.; Hung, C.-H. *Inorg. Chem.* **2001**, *40*, 5070.
(30) Rachlewicz, K.; Wang, S.-L.; Peng, C.-H.; Hung, C.-H.; Latos-Grażyński, L. *Inorg. Chem.* **2003**, *42*, 7348.
(31) Rachlewicz, K.; Wang, S.-L.; Ko, J.-L.; Hung, C.-H.; Latos-Grażyński, L. *J. Am. Chem. Soc.* **2004**, *126*, 4420.
(32) Walker, F. A. Proton NMR and EPR Spectroscopy of Paramagnetic Metalloporphyrins. In *The Porphyrin Handbook*; Kadish, K. M., Smith, K. M., Guilard, R., Eds.; Academic Press: San Diego, CA, 2000; pp 81−183.
(33) Wojaczyński, J.; Latos-Grażyński, L. *Inorg. Chem.* **1995**, *34*, 1044.
(34) Wojaczyński, J.; Latos-Grażyński, L.; Olmstead, M. M.; Balch, A. L. *Inorg. Chem.* **1997**, *36*, 4548.

Scheme 1. Synthesis of Iron(II) N-confused Pyriporphyrin Complexes

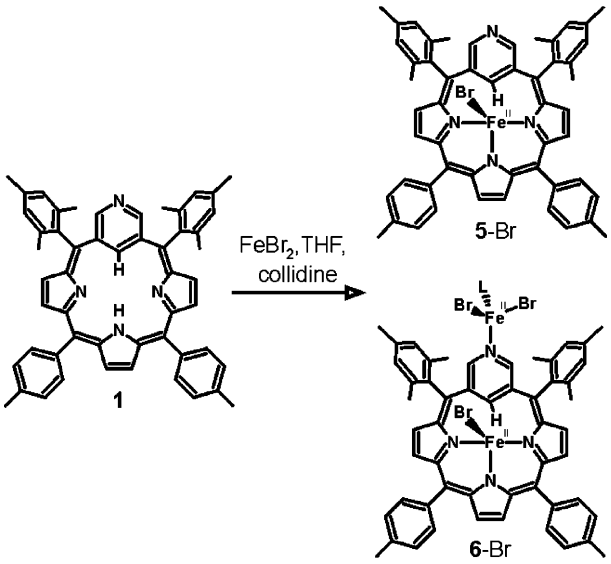

ziporphyrin **1** has been achieved by addition of iron(II) bromide to a THF solution of the ligand under strictly anaerobic conditions. Iron(II) bromide (free of iron(II)) was prepared by stirring anhydrous iron(II) bromide and an excess of iron powder in THF. This reduction step is essential for metalation as the residual iron(III) can be involved in side reactions with the products of insertion. The insertion yield is quantitative with respect to **1**. Actually, two products have been identified using the ^{1}H NMR spectroscopy. The marked difference of their solubility in toluene allowed their straightforward separation. The resulting complexes will be denoted **5**-Br and **6**-Br (Scheme 1). A similar procedure yielded **5**-Cl as a single product once hydrated $FeCl_2$ was applied.

The ESI mass spectrum of **5**-Br shows the small peak corresponding to a parent species (PyP*H*)Fe^{II}Br **5**-Br at m/z = 872.5. The most intense peak at m/z = 793.5 is from the dissociation of a bromide ligand from (PyP*H*)Fe^{II}Br forming a cation [(PyP*H*)Fe^{II}]$^+$. The ESI spectrum of **6**-Br, when dissolved in chloroform/methanol, yielded the most intense peak at m/z = 1074.8 which corresponds to the formula {[Fe^{II}Br$_2$(CH$_3$OH)]-[(PyP*H*)Fe^{II}(CH$_3$OH)]}$^+$, **6**-(CH$_3$OH)$^+$. From **6**-Br in Scheme 1, this observation is consistent with a substitution of the bromide ligand of [(PyP*H*)Fe^{II}Br] with methanol (L = CH$_3$OH). The tetrahedral coordination geometry around the external iron(II) is suggested.

The electronic spectrum of **5**-Br resembles that of iron(II) benziporphyrin (Figure 1).[17] The coordination of iron(II) to the external nitrogen of **5**-Br is reflected in particular by a new band at 649 nm. The reaction of **5**-Br and **6**-Br with dioxygen, which yielded **7**-Br, has been followed using UV−vis spectroscopy. The relatively slow reaction of **5**-Br with dioxygen is in contrast to the fast oxygenation of iron(II) N-confused porphyrin.[31]

NMR Studies of Iron(II) N-Confused Pyriporphyrin. The molecular structure of **5**-Br is expected to be analogous to those of the X-ray characterized metallobenziporphyrins[15−17] because the external nitrogen atom is expected to play a minor role in the structural preferences (Figure 2). The

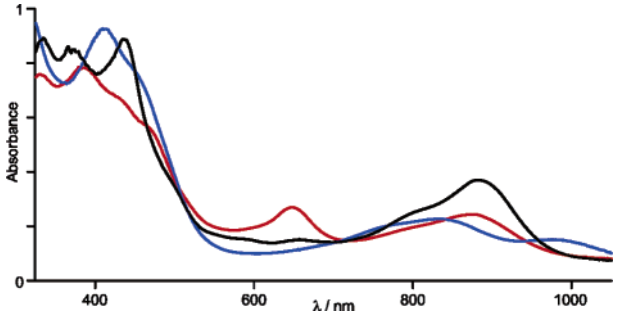

Figure 1. Electronic spectrum of **5**-Br (black line, in toluene), **6**-Br (red line, in dichloromethane), and **7**-Br (blue line, in dichloromethane).

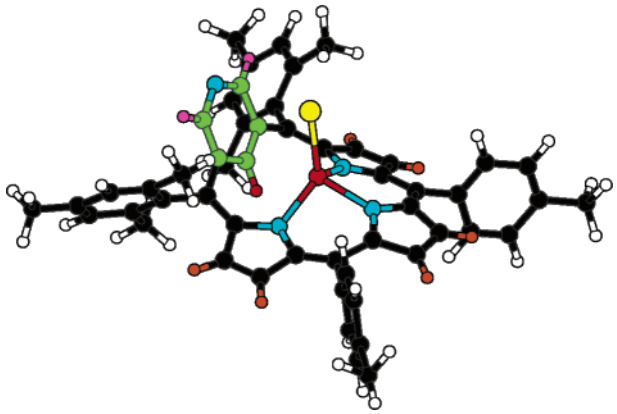

Figure 2. Drawing of the **5**-Br structure obtained from the molecular mechanics calculations.

coordinating environment of the metal ion forms a trigonal bipyramid, with the N(24) atom, anionic ligand, and the C(22)−H bond occupying the equatorial positions. In the absence of X-ray data, molecular mechanics calculations have been used to visualize the structure of **5**-Br in the minimization procedure using the standard MM+ parametrization with exception of the iron coordination surroundings. Namely, constraints have been imposed which reflect iron−nitrogen bond lengths typical for high-spin state iron(II) porphyrinoids.[17,29,35]

The ^{1}H NMR spectrum of **5**-Br, corresponding to the effective C_s symmetry of the molecule, is consistent with the structure shown in Figure 2. The mirror plane goes through the Br, Fe, and N(24) atoms. There are three distinct β-H pyrrole positions, two pyridine H(2/4) and H(22) positions, and two different *meso*-aryls.

The pertinent spectral parameters have been gathered in Table 1. Resonance assignments, which are given above selected peaks, have been made on the basis of relative intensities, line widths, and pyrrole specific deuteration. The line widths were compared for the spectra collected at 233 K to avoid any problems resulting from the feasible exchange-related broadening. The observed pattern of chemical shifts of **5**-X is quite typical for high-spin iron(II) porphyrins and porphyrin analogues with three β-pyrrole resonances in the region from 60 to −2 ppm and the *meso*-aryl peaks in the 15 to −5 ppm range.[30−32,36−38] The relatively large line widths of *meso*-phenyl resonances as compared

(35) Latos-Grażyński, L.; Lisowski, J.; Olmstead, M. M.; Balch, A. L. *Inorg. Chem.* **1989**, *28*, 1183.

Table 1. ^{1}H NMR Chemical Shifts[a] of Iron N-confused Pyriporphyrins

complex	solvent	H(22)[b]	H(2/4)	pyrrole		
5-Br	C_7D_8	424.6 (4600)	54.3	50.8	24.5	−1.2
5-Cl	$CDCl_3$	416.6 (4760)	52.4	48.7	22.9	−1.0
5-(THF-d_8)	THF-d_8	468.8 (4560)	64.3	44.0	25.0	−1.5
5-(CD_3CN)	CD_3CN	502.2 (4030)	70.1	46.0	23.4	−1.0
5-(CD_3OD)	CD_3OD	758 (11700)	63.5	53.6	45.0	*c*
6-Br	CD_2Cl_2	375.3 (2500)	201.3	57.2	53.6	0.7

[a] All data in ppm at 298 K. [b] Line widths (Hz) in parentheses. [c] Not identified.

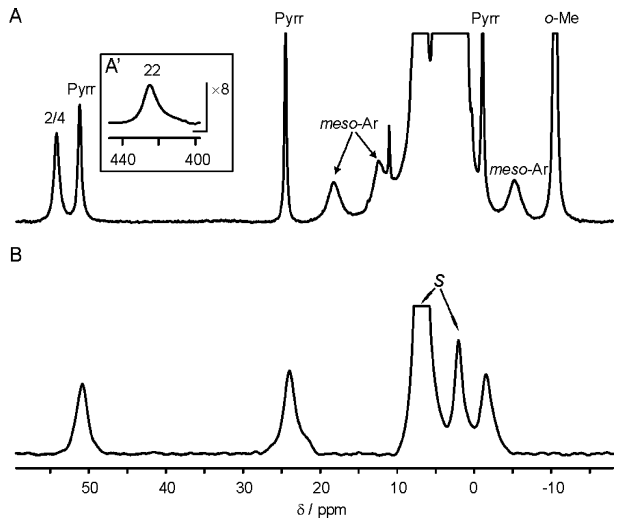

Figure 3. NMR spectra: (A) **5**-Br (^{1}H NMR, toluene-d_8, 298 K); (B) **5**-Br-d_6 (^{2}H NMR, toluene, 298 K). The inset (A′) presents the H(22) peak.

to β-H ones reflect the rotation of *meso*-aryls (Figure 3).[32] The hydrogens on the *m*-pyridyl ring have been identified by default. Interestingly, ∼420 ppm shift of the inner C(22)−H proton is similar to that of iron(II) *m*-benziporphyrin[17] but much smaller than the corresponding H(21) shift determined for iron(II) N-confused porphyrin (812 ppm, 298 K).[30] A similar value has been found value for nickel(II) *m*-benziporphyrin (386 ppm, 298 K).[15] An agostic mechanism of spin-density transfer, described previously for nickel(II) *m*-benziporphyrin, explains the shifts of **5**-X as resulting from electron donation from the CH bond to the metal. The addition of small amount of acid to **5**-Br in toluene-d_8 gave rise to the strongly upfield resonances at −72.7 ppm (298 K) assigned to NH hydrogen of protonated pyridine. The plots of the temperature dependence of the chemical shifts (Figure 3S, Supporting Information) demonstrated the features typical for high-spin iron(II) porphyrinoids.[30]

(PyP*H*)Fe^{II}Br, **5**-Br, once dissolved in coordinating solvents, yields the high-spin five-coordinate species [(PyP*H*)-Fe^{II}L]$^+$, **5**-L (L = THF-d_8, acetonitrile-d_3, methanol-d_4). The solvent coordination produces visible changes in positions of the selected resonances (Table 1), but the overall ^{1}H NMR features assigned to high-spin iron(II) N-confused pyriporphyrin are preserved. In particular, the dramatic relocation of the H(22) resonance from 424.6 to 758 ppm (298 K)

Scheme 2. Equilibrium between **5**-L and **6**-L (L = Cl or solvent) in Coordinating Solvent

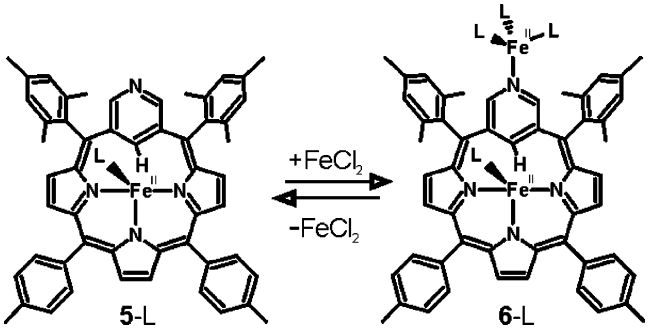

because of the replacement of bromide ligand by methanol has been noticed.

Titration with Paramagnetic Metal(II) Ions. To probe the coordination ability of the perimeter nitrogen to bind iron(II), systematic titration of (PyP*H*)Fe^{II}Cl, **5**-L, in acetonitrile-d_3 or THF-d_8 has been carried out. In the course of titration of (PyP*H*)Fe^{II}Cl with Fe^{II}Cl$_2$, smooth changes of the chemical shifts of the pyridine moiety were noticed, indicating that it was directly engaged in coordination. Under these experimental conditions, the reaction involves solvated forms such as [(PyP*H*)Fe^{II}L]$^+$, **5**-L, **6**-L, and Fe^{II}L$_n$, respectively (Scheme 2).

The detected chemical shifts are the time-averaged values, which reflect relative populations of the mono- and diiron species (**5**-L−**6**-L), which are in fast exchange. In the final stage of titration, determined by the solubility of iron(II) in acetonitrile-d_3, the H(2/4) and H(22) resonances have been located at 123 and 489 ppm, respectively, which is a remarkable relocation with respect to the starting values (70 ppm for H(2/4) and 502 ppm for H(22)). Smaller changes following the same directions were determined in THF-d_8. An analogous titration of **5**-L with cobalt(II) chloride in acetonitrile-d_3 resulted in a pattern similar to that described for iron(II) in the same solvent. All titrations were carried out in anaerobic conditions. Once dioxygen was added to the sample containing **6**-L, the spectroscopic changes initially reflected the reconversion to **5**-L. Presumably, the oxidation of the external iron(II) to iron(III) resulted in its dissociation from **6**-L. Under these experimental conditions, the affinity of iron(III) to N(3) of pyridine seems to be smaller than that of iron(II).

Diiron Species 6. The titration experiment set some limits the ^{1}H NMR spectroscopic range expected for the diiron species **6** in the slow exchange limits (i.e., under conditions created in a chlorinated solvent). The ^{1}H NMR spectrum of the detected diiron compound **6**-Br is presented in Figure 4.

The spectroscopic pattern of **6**-Br resembles that of the monoiron species **5**-L with one but crucial addition. Consequently, the H(2/4) hydrogen yields a remarkably shifted resonance at 201 ppm (298 K) (Figure 4). Actually, this resonance is located in the region which is consistent with the titration data presented previously. The ^{1}H NMR spectra of pyridine coordinated to a high-spin metal ion with half-occupied d_{z^2}, which may serve as the reference point to assign H(2/4) are difficult to generate because of the intrinsic lability

(36) Balch, A. L.; Chan, Y.-W.; La Mar, G. N.; Latos-Grażyński, L.; Renner, M. W. *Inorg. Chem.* **1985**, *24*, 1437.
(37) Pawlicki, M.; Latos-Grażyński, L. *Inorg. Chem.* **2002**, *41*, 5866.
(38) Pawlicki, M.; Latos-Grażyński, L. *Inorg. Chem.* **2004**, *43*, 5564.

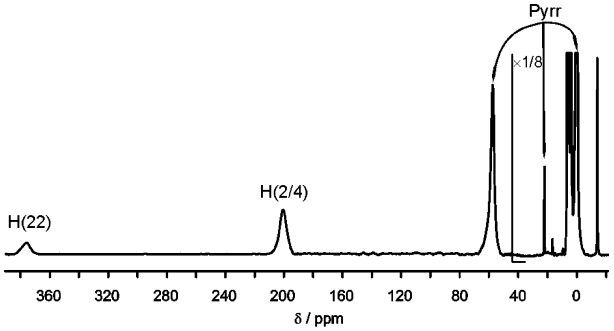

Figure 4. Composite ^{1}H NMR spectrum of **6**-Br (dichloromethane-d_2, 298 K). Labels as in Chart 1. This figure was composed from three spectra collected over the following regions: 160 to −40, 245 to 45, and 380 to 180 ppm. The frequency domain spectra were subsequently added, preserving the relative intensities of the resonances.

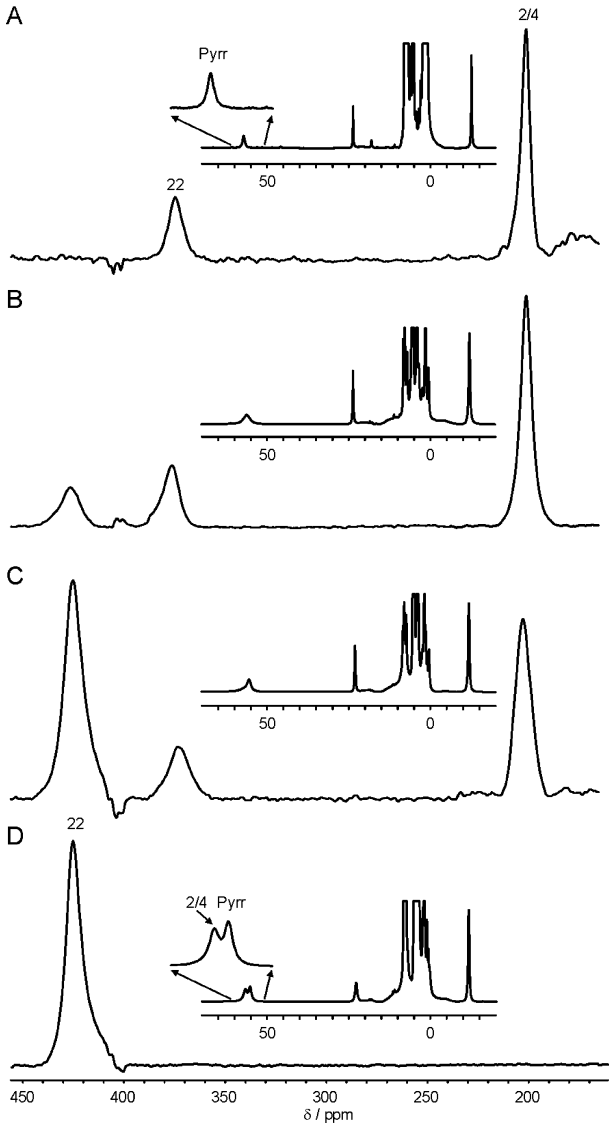

Figure 5. Composite ^{1}H NMR spectra showing a conversion of **6**-Br (dichloromethane-d_2, 298 K) into **5**-Br in the course of titration with Br_2 (5 μL/200 μL solution in dichloromethane-d_2). Trace A shows the spectrum of **6**-Br separated from the insertion products by extraction of **5**-Br with toluene. Trace B shows the mixture of **5**-Br and **6**-Br as obtained directly in synthesis. Traces C and D show the effects of additions of 4 μL (C) and 6 μL (D) of the Br_2 solution to the original sample shown in B. To generate the figure, the frequency domain spectra were subsequently added, preserving the relative intensities of the resonances. The insets present the 70 to −20 ppm region of the appropriate spectrum.

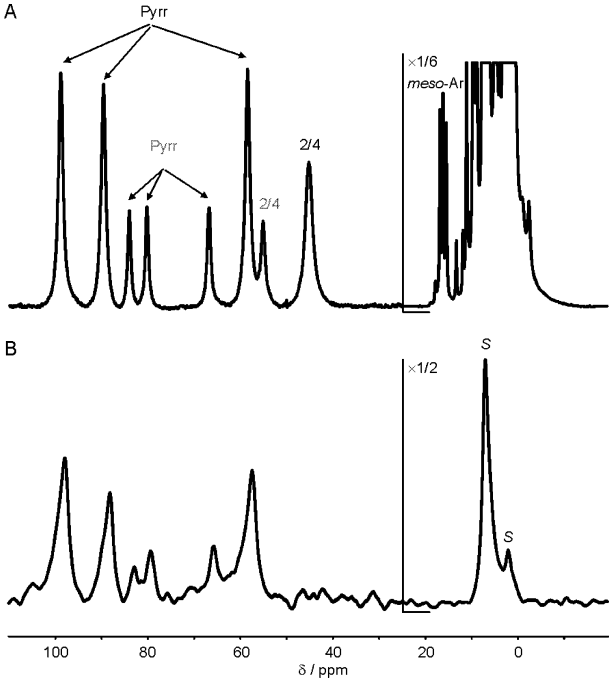

Figure 6. NMR spectra: (A) **7a**-Br (black labels) and **7b**-Br (gray labels) formed by the addition of dioxygen to **5**-Br (^{1}H NMR, toluene-d_8, 298 K) and (B) **7a**-Br-d_6 and **7b**-Br-d_6 (^{2}H NMR, toluene, 298 K).

of the formed compounds and the rather large shifts and line widths expected for the α-*H*-pyridine resonances. Previously it was determined that pyridine, axially coordinated to nickel(II) thiaporphyrin, revealed the following pattern: H(2) 156.3, H(3) 68.4, H(4) 17.2 ppm (203 K, dichloromethane-d_2).[39] The downfield position of H(2/4) resonance for **6**-Br is consistent with coordination to the high-spin iron(II), assuming that the spin delocalization pathways are identical with that determined for nickel(II) thiaporphyrin.

6-Br can be easily converted in the derivative of **5**-X via the addition of competing ligands or external iron(II) directed oxidation. The addition of pyridine-d_5 to the solution of **6**-Br in dichloromethane-d_2, as followed by ^{1}H NMR, removed its H(2/4) resonance from the spectrum because of the formation of **5**-Br and the iron(II)−pyridine-d_5 complex. The ^{1}H NMR titration of **6**-Br with bromine is shown in Figure 5. The selected region covers H(2/4) resonance of **6**-Br and H(22) resonances of **5**-Br and **6**-Br. The overlapping pyrrole and H(2/4) resonances of **5**-Br and **6**-Br are shown in insets (traces B, C, and D). Throughout the entire titration, a single set of resonances has been detected for all β-H positions, which reflects the fact that **5**-Br and **6**-Br are in fast exchange in this particular spectroscopic window. At the same time, two separate H(22) resonances have been detected as the chemical shift difference are markedly large for **5**-Br and **6**-Br for these particular hydrogens. Actually, the individual H(2/4) resonances assigned for **5**-Br and **6**-Br have been clearly identified throughout the whole titration. Despite the enormous line widths, the far downfield-shifted resonances provide the very valuable analytical pattern, which is unique for the N-confused pyriporphyrin diiron species **6**-Br.

(39) Chmielewski, P. J.; Latos-Grażyński, L. *Inorg. Chem.* **1992**, *31*, 5231.

Scheme 3. Oxidation and Oxygenation of **5**-Br

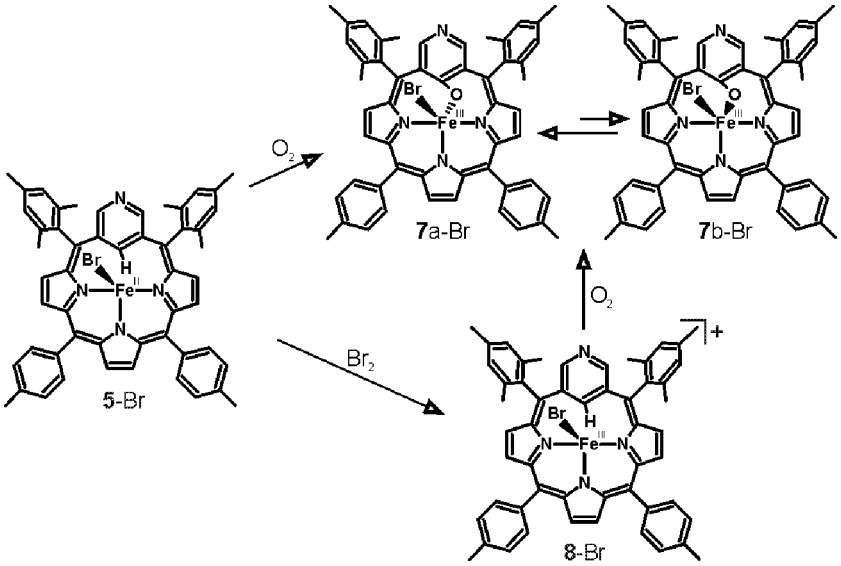

Chart 2. Structure of **9**-Br

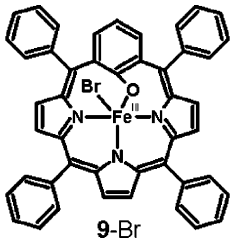

Oxidation and Oxygenation of 5-Br. The reaction of (PyP*H*)Fe^{II}Br, **5**-Br, with dioxygen (72 h in toluene-d_8) results in the formation of a five-coordinate species (PyPO)Fe^{III}Br, **7**-Br ((PyPOH)H 3-aza-22-hydroxy-*m*-benziporphyrin, PyPO $-$ the corresponding dianion). **7**-Br is formed by oxygenation at the C(22) position (Scheme 3).

In the course of this process, the new type of core-modified porphyrin was identified. The macrocycle incorporates a 4-hydroxypyridine unit into the porphyrin-like structure. **7**-Br is stable and was purified by the standard chromatographic procedure. Actually, the ^{1}H NMR spectroscopic features of **7**-Br reproduce those of the iron(III) core modified porphyrin incorporating a phenolate donor **9**[40] (Chart 2), with the H(3) resonance missing from the spectrum as the corresponding CH unit was replaced in **7**-Br by nitrogen. The compound **7**-Br is actually a mixture of two isomers (Scheme 3). They will be denoted **7a**-Br and **7b**-Br with isomer **7a**-Br being more abundant. Two sets resonances in the downfield region of the spectrum, each composed of three pyrrole and one 2/4-H resonances of the pyridinolato fragment, allowed their identification. Relative amounts of the two isomers were estimated by careful deconvolution of the downfield region of the spectrum. The concentration ratio [**7a**-Br]/[**7b**-Br] equals 3.5 (298 K, toluene-d_8).

Coordination of a metal ion by 3-aza-22-hydroxybenziporphyrin imposes a steric constraint on the geometry of the ligand. In analogy to **9**,[40] the pyridinolato moiety of **7**-Br is expected to be positioned at an angle to the macrocyclic plane. Thus, in the ferric **7**-Br complexes, the halide ligand can be coordinated on one of the two inequivalent faces of the macrocycle, leading to two distinct species (syn and anti). A similar type of isomerism was previously observed for the 22-hydroxybenziporphyrin complexes and asymmetric metalloporphyrin derivatives.[41−43] The shift pattern demonstrated by the pyridinolato moiety is of particular significance, revealing the downfield positions of H(2/4) for **7a** and **7b**. This ^{1}H NMR position is very characteristic for a phenoxide ligand coordinated to iron(III) porphyrins and porphyrinoids.[44]

A careful titration of (PyP*H*)Fe^{II}Br, **5**-Br, with Br_2 has been carried out in dichloromethane-d_2. The characteristic set of three pyrrole resonances at 122.4, 79.6, and 70.4 ppm (dichloromethane-d_2, 298 K) assigned to [(PyP*H*)Fe^{III}Br]$^+$, **8**-Br (i.e., to the product of one-electron metal-centered oxidation of (PyP*H*)Fe^{II}Br, **5**-Br). Significantly, the fast conversion of [(PyP*H*)Fe^{III}Br]$^+$, **8**-Br, into (PyPO)Fe^{III}Br, **7**-Br. in the presence of dioxygen takes place.

Conclusions. This study broadens our understanding of the coordination of iron in a porphyrin and in porphyrin−like environments. Essential similarities of iron N-confused porphyrin and iron N-confused pyriporphyrin complexes have been established. There is a considerable analogy in their ^{1}H NMR properties. Significantly, the nitrogen atom at the macrocyclic perimeter may provide a promising means to control overall macrocyclic properties, for instance, via protonation or alkylation. Potentially, an external N-coordination of pyridine offers a route to construct polymetallic arrays where the pyridine moiety will serve as a unique bridge, which links two metal ions, involving a simultaneous

(40) Stępień, M.; Latos-Grażyński, L. *Inorg. Chem.* **2003**, *42*, 6183.

(41) Balch, A. L.; Latos-Grażyński, L.; Noll, B. C.; Olmstead, M. M.; Zovinka, E. P. *Inorg. Chem.* **1992**, *31*, 2248.

(42) Kalish, H.; Camp, J. E.; Stępień, M.; Latos-Grażyński, L.; Olmstead, M. M.; Balch, A. L. *Inorg. Chem.* **2002**, *41*, 989.

(43) Tung, J.-Y.; Jiang, J.-I.; Lin, C.-C.; Chen, J.-H.; Hwang, L.-P. *Inorg. Chem.* **2000**, *39*, 1.

(44) Arasasingham, R. D.; Balch, A. L.; Hart, R. H.; Latos-Grażyński, L. *J. Am. Chem. Soc.* **1990**, *112*, 7566.

coordination by the C (CH or CO) and N ends of pyridine. Actually, the design of discrete ordered patterns of porphyrins and metalloporphyrins has attracted much interest recently leading to the synthetic methodology with a "building block" approach.[45−50] The oligomeric porphyrins and metalloporphyrins of various structures are under intensive investigation because of their potential applications in molecular electronics and as new photonic materials.[51,52] Previously, several polymeric or oligomeric metalloporphyrin structures, obtained by a self-assembly approach, were constructed employing a *meso*-pyridyl moiety coordination.[47,48,53,54] In this context, the coordinating properties of N-confused pyriporphyrin, containing a pyridyl moiety directly built into the porphyrin frame, are of further interest.

Experimental Section

Materials. N-confused pyriporphyrin was obtained by previously described methods.[1] The deuterated derivatives were synthesized using pyrrole-d_5 and trifluoroacetic anhydride/D_2O in a condensation to give a sample of N-confused pyriporphyrin which was shown by ^{1}H NMR spectroscopy to be maximally 50% deuterated at the pyrrolic positions.

Toluene-d_8 (distilled under nitrogen from sodium), tetrahydrofurane-d_8, dichloromethane-d_2, chloroform-d, and acetonitrile-d_3 were degassed by the freezing−pumping−thawing method and stored in a dry glovebox.

Iron(II) Insertion into N-Confused Pyriporphyrin: 5-Br and 6-Br. Iron(II) bromide (free of iron(III)) was prepared by stirring under N_2 (in a glovebox) 0.043 g (0.2 mmol, 5 equiv) of anhydrous iron(II) bromide and excess (∼0.07 g) iron powder in ∼4 mL THF (distilled from sodium under N_2) until the solution became colorless. Iron was filtered off, and the colorless solution of iron(II) bromide was added to a dark green THF solution of **1** (0.03 g, 0.04 mmol). An aliquot of ∼5 μL of collidine was added. The resulting brownish solution was heated and stirred at 55 °C for 3 h. The iron insertion was quantitative, as confirmed by ^{1}H NMR. The solution was evaporated and dried in a glovebox. The residue was redissolved in a minimum volume of toluene. The marked solubility difference in toluene allowed straightforward separation of **5**-Br and **6**-Br. The solid **6**-Br was filtered off. The toluene solution was dried under vacuum to obtain species **5**-Br.

5-Br. HRMS (ESI, *m*/*z*): $[M - Br]^+$ 793.2894 (793.2994 calcd for $C_{53}H_{45}N_4{}^{56}Fe^+$). UV−vis ($\lambda_{max}$, nm): 335, 373, 436, 881.

6-Br. Dissolved in CH_2Cl_2/CH_3OH. MS (ESI, *m*/*z*): 1073.8 (calcd 1073.5 for $[C_{55}H_{53}N_4O_2{}^{79}Br^{81}Br^{56}Fe_2]^+$ which corresponds to $\{[Fe^{II}Br_2(CH_3OH)]$-$[(PyP\mathit{H})Fe^{II}(CH_3OH)]\}^+$). UV−vis ($\lambda_{max}$, nm): 330, 385, 385, 649, 875.

7-Br. A dichloromethane or toluene solution of **5**-Br (3 mg in 1 mL of solvent) was purged with dioxygen for 15 min. Subsequently, **7**-Br was separated using column chromatography on silica. The fraction eluted with acetone, containing **7**-Br, was collected and evaporated. HRMS (ESI, *m*/*z*): $[M - Br]^+$ 808.2882 (calcd 808.2866 for $[C_{53}H_{44}N_4O^{56}Fe]^+$). UV−vis ($\lambda_{max}$, nm): 412, 832, 978.

^{1}H NMR Studies. The solution of **5**-Br or **6**-Br in a deuterated solvent was prepared under purified nitrogen in a glovebox. Typically a sample of ∼1−2 mg of **5**-Br or **6**-Br was dissolved in 0.5 mL of deuterated solvent. The solution was directly placed into an ^{1}H NMR tube and sealed with a septum cap. In titration experiments, a solution of the pyridine-d_5 or oxidizing reagent in the deuterated, deoxygenated solvent was gradually added to the sample through a 10 μL microsyringe. Usually an appropriate mass of the applied reagent was dissolved to give an approximately 0.25 M solution. It typically required 2−5 μL of the solution to be added to the NMR tube containing iron N-confused pyriporphyrin to cause a detectable conversion. The addition of dioxygen was carried out by purging of oxygen through the sample.

^{2}H NMR Studies. The samples used in ^{2} H NMR experiments have been prepared similarly as those for ^{1}H NMR starting from **5**-Br-d_6 or **6**-Br-d_6 using regular solvents.

Instrumentation. ^{1}H NMR 500 MHz spectra were measured on Bruker Avance 500 spectrometers. The peaks were referenced against the residual resonances of the deuterated solvents. The ^{2}H NMR spectra were collected using a Bruker Avance 500 instrument operating at 76.77 MHz. A spectral width of 200 ppm was typical and 32 K points were used. A pulse delay of 50 or 100 ms was applied. The residual ^{2}H NMR resonances of the solvents were used as a secondary reference.

Molecular Mechanics Calculation. Molecular mechanics calculations were performed using the HyperChem software (Autodesk). The standard MM+ force field, with the constraints set on the coordination bonds to achieve a high-spin iron(II) porphyrin geometry, were used as described in the text.

Acknowledgment. This work was supported by the Ministry of Scientific Research and Information Technology of Poland under Grant 3 T09A 162 28.

Supporting Information Available: MS spectra for $\mathbf{5}^+$, $\mathbf{6}^+$, and $\mathbf{7}^+$ and VT NMR data for **5**-Br and **6**-Br. This material is available free of charge via the Internet at http://pubs.acs.org.

IC060906R

(45) Burrell, A. K.; Officer, D. L.; Plieger, P. G.; Reid, D. C. *Chem. Rev.* **2001**, *101*, 2751.
(46) Burrell, A. K.; Wasielewski, M. R. *J. Porphyrins Phthalocyanines* **2000**, *4*, 401.
(47) Imamura, T.; Fukushima, K. *Coord. Chem. Rev.* **2001**, *198*, 133.
(48) Wojaczyński, J.; Latos-Grażyński, L. *Coord. Chem. Rev.* **2000**, *204*, 113.
(49) Prodi, A.; Indelli, M. T.; Kleverlaan, C. J.; Alessio, E.; Scandola, F. *Coord.Chem. Rev.* **2002**, *229*, 51.
(50) Iengo, E.; Zangrando, E.; Bellini, M.; Alessio, E.; Prodi, A.; Chiorboli, C.; Scandola, F. *Inorg. Chem.* **2005**, *44*, 9752.
(51) Benniston, A. C. *Chem. Soc. Rev.* **2004**, *33*, 573.
(52) Drain, C. M.; Goldberg, I.; Sylvain, I.; Falber, A. *Top. Curr. Chem.* **2005**, *245*, 55.
(53) Drain, C. M.; Nifiatis, F.; Vasenko, A.; Batteas, J. D. *Angew. Chem., Int. Ed. Engl.* **1998**, *37*, 2344.
(54) Drain, C. M.; Lehn, J. *J. Chem. Soc., Chem. Commun.* **1995**, 503.